Leucine-rich repeat–containing G-protein–coupled receptor 5–positive cells in the endometrial stem cell niche

Irene Cervelló, Ph.D.,[a] Claudia Gil-Sanchis, Ph.D.,[a] Xavier Santamaría, Ph.D., M.D.,[a,b,c] Amparo Faus, B.Sc.,[a] Julia Vallvé-Juanico, Ph.D.,[b,c] Patricia Díaz-Gimeno, Ph.D.,[a] Oriana Genolet, Ph.D.,[a] Antonio Pellicer, Ph.D., M.D.,[a] and Carlos Simón, Ph.D., M.D.[a,d]

[a] Fundación Instituto Valenciano de Infertilidad, Department of Obstetrics and Gynecology, School of Medicine, Valencia University and Instituto Universitario IVI/INCLIVA, Valencia; [b] IVI Barcelona, Reproductive Medicine Department, Barcelona; [c] Vall Hebron Institut de Recerca, Biomedical Research Group in Gynecology, Barcelona, Spain; and [d] Department of Obstetrics and Gynecology, Stanford University School of Medicine, Stanford University, Stanford, California

Objective: To study, isolate and characterize leucine-rich repeat–containing heterotrimeric guanine nucleotide–binding protein–coupled receptor 5 (LGR5)–positive cells from human endometrium to determine their functional relevance.
Design: Prospective experimental animal study.
Setting: University research laboratories.
Animal(s): Nonobese diabetic mice (NOD-SCID) (strain code 394; NOD.CB17—Prkdc^{scid}/NcrCrl).
Intervention(s): Human LGR5^{+} cells were labeled with superparamagnetic iron oxide nanoparticles (SPIOs) and injected under the kidney capsule in immunocompromised mice.
Main Outcome Measure(s): Epithelial and stromal LGR5^{+} cells were isolated from human endometrium by means of fluorescence-activated cell sorting, and phenotypic characterization was performed by means of flow cytometry with the use of hematopoietic and mesenchymal markers. Engrafted SPIO-labeled LGR5^{+} cells were localized with the use of Prussian blue staining and immunohistochemistry against CD9 and Vimentin. Deep transcriptomic profiling of LGR5^{+} cells was performed with the use of microarrays and RNA sequencing.
Result(s): The percentage of LGR5^{+} cells in human endometrium represented 1.08 ± 0.73% and 0.82 ± 0.76% of total cells in the epithelial and stromal compartments, respectively. LGR5^{+} cells were phenotypically characterized by abundant expression of CD45 hematopoietic marker and no expression of surface markers CD31, CD34, CD133, CD73, and CD90. Coexpression with the macrophage marker CD163 was detected. Xenotransplantation of labeled LGR5^{+} cells into the kidney capsules of immunocompromised mice resulted in a weak endometrial reconstitution from this cell of origin. Transcriptomic profiling revealed new attributes for LGR5^{+} cells related to their putative hematopoietic origin.
Conclusion(s): These data suggest that endometrial LGR5 is not an endogenous stem cell marker. Instead, LGR5^{+} cells appear to be recruited from blood to be part of the stem cell niche at the perivascular microenvironment to activate the endogenous niche. (Fertil Steril® 2017;107:510–9. ©2016 by American Society for Reproductive Medicine.)
Key Words: Somatic stem cells, human endometrium, stem cell marker, LGR5, hematopoietic lineage

Discuss: You can discuss this article with its authors and with other ASRM members at https://www.fertstertdialog.com/users/16110-fertility-and-sterility/posts/12648-22972

Received August 23, 2016; revised October 13, 2016; accepted October 14, 2016; published online November 22, 2016.
I.C., C.G.-S., and X.S. should be considered similar in author order.
I.C. has nothing to disclose. C.G.-S. has nothing to disclose. X.S. has nothing to disclose. A.F. has nothing to disclose. J.V.-J. has nothing to disclose. P.D.-G. has nothing to disclose. O.G. has nothing to disclose. A.P. has nothing to disclose. C.S. has nothing to disclose.
Supported by Leonardo scholarship (O.G.) SAF2012-31017, Generalitat Valenciana GV/2013/120, and PROMETEOII/2013/018.
Reprint requests: Irene Cervelló, Ph.D., Fundación IVI (Parc Científic Universitat de València), Calle/Catedrático Agustín Escardino no 9, Edificio 3, Paterna, Valencia 46980, Spain (E-mail: irene.cervello@ivi.es).

Fertility and Sterility® Vol. 107, No. 2, February 2017 0015-0282/$36.00

http://dx.doi.org/10.1016/j.fertnstert.2016.10.021

The endometrium is a dynamic tissue with an extraordinary regenerative capacity throughout a woman's reproductive life (1, 2). Somatic stem cells (SSCs), represented mostly by the side population (SP), have been proposed as the endogenous cellular source responsible for this exceptional regenerative ability (3, 4) and are extensively characterized in the human endometrium (5–9). However, SP cells are heterogeneous; therefore, the search for specific stem cell markers to characterize the human endometrial SSC population continues. Several candidates have been proposed, such as CD146 and PDGFR-beta (10), Musashi-1 (11), and W5C5 (12), but no consistent agreement has been reached and no markers have been translated to the clinic.

The identification of the self-renewing capacity of small intestinal mucosa revealed specific genes with expression restricted to the intestinal crypt bottom (13). The most important, termed leucine-rich repeat–containing heterotrimeric guanine nucleotide–binding protein–coupled receptor 5 (LGR5), is a cell surface receptor that is activated to trigger canonic Wnt signaling. Heterozygous *Lgr5-LacZ* mice revealed an active cycling nature, long life, and multipotent ability in cells expressing LGR5; all of these features are characteristic of stem cells (14). LGR5 is currently considered to be a murine SSC marker because of its presence not only in small intestine, but also in colon and stomach (15). Each of these tissues originates from endoderm, but LGR5 has also been detected in nonendodermal derived tissues such as hair follicle (ectoderm origin) (16) and kidney (mesoderm origin) (17).

Thus, the presence of LGR5$^+$ cells in several tissues is correlated with stem cell maintenance, differentiation, and tissue homeostasis. Surprisingly, LGR5 is detected in human endometrium at the mRNA (18, 19) and protein (19) levels, and the LGR5$^+$ cell population is localized at the perivascular niche in the lower functionalis region (19). It has been suggested that the niche for endometrial SSCs could be the perivascular region of the endometrium (20). Therefore, the implication of LGR5 as stem cell marker in human endometrium has been proposed several times, but functional proof remains elusive.

We hypothesized that LGR5 may be an SSC marker in tissues derived not only from endoderm or ectoderm, but also from mesoderm, making it a potentially universal SSC marker. In the present work, we aimed to demonstrate whether LGR5 could be a tissue-specific SSC marker in human endometrium. For this purpose, we isolated and phenotyped LGR5$^+$ cells from the human endometrium. As a functional proof of concept, labeled LGR5$^+$ cells were injected into the kidney capsule of immunocompromised mice to verify their putative regenerative ability. We also attempted to elucidate their origin and role in the human endometrial niche based on their specific cell phenotype and the functional gene expression characterization. These findings have implications for furthering our understanding of the endometrial stem cell niche.

MATERIAL AND METHODS

Human Tissue Collection

Use of human tissue specimens was approved by the ethics committee of the Instituto Valenciano de la Infertilidad (IVI) (Number: 1203-C-098-IC-F).

Isolation of Endometrial LGR5$^+$ Cells

Epithelial and stromal cell separation. Endometrial biopsies from donors were obtained on the day of oocyte collection; a total of 13 samples were collected for different experiments (n = 3 for phenotypic analysis; n = 3 for the animal model; n = 4 for microarray assays; and n = 3 for RNA sequencing). Samples were carefully rinsed of blood and mucus and sliced into 1–2-mm^3 fragments. Digestion was carried out in Dulbecco modified Eagle medium (DMEM; Sigma-Aldrich) containing 10 mg collagenase type IA (Sigma-Aldrich). Epithelial and stromal cells were separated based on their size by means of gravity sedimentation and membrane filtration, as previously described, and subsequently treated with standard erythrocyte lysis solution (21).

Sorting of human endometrial LGR5$^+$ cells. Samples were incubated with the polyclonal rabbit anti-human antibody against the LGR5 antigen (Novus 28904; 1 μL per million of cells) in phosphate-buffered saline solution (PBS; Gibco Life Technologies) containing 3% bovine serum albumin (BSA) for 1 hour at 4°C on ice. Cells were incubated with secondary antibody (goat anti-rabbit, A11034, 1:500, Alexa 488; Life Technologies) for 45 minutes at 4°C. Cells were then washed with PBS and resuspended in Hank balanced salt solution buffer (Gibco Life Technologies). Epithelial and stromal cell suspensions were filtered through 50 μm and 30 μm pore-size filters, respectively (Partec; Celltrics).

Fluorescence-activated cell sorting (FACS) was used to isolate LGR5$^+$ cells (for flow cytometry and transcriptomic analysis) or LGR5$^+$/Rhodamine$^+$ (for xenotransplantation). To detect and distinguish LGR5-Alexa 488 and Rhodamine B simultaneously, a Moflo Legacy high-speed cell sorter (Beckman-Coulter) was used. The signals for LGR5-Alexa 488 and Rhodamine B were acquired using the 525 nm and 620 nm channels, respectively, after excitation by means of the 488 nm laser. A 6-diamino-2-phenylindole (DAPI) probe (5 μg/mL) was used to discard dead cells, which were detected in the 450 nm channel after excitation by means of the 351 nm laser. Live cells (DAPI$^-$ cells) were gated in an FS/DAPI dot plot and applied to the LGR5-Alexa 488/Rhodamine B dot plot, where double-positive cells were selected for cell sorting.

Phenotypic analysis of human endometrial LGR5$^+$ cells. Epithelial and stromal LGR5$^+$ cells were washed and then incubated for 45 minutes at 4°C with the following antibodies: mouse anti–human CD9-PE (eBioscience), mouse anti–human CD13-PE (BD Biosciences), mouse anti–human CD31-PE (Abcam), mouse anti–human CD34-PECy5 (BD Biosciences), mouse anti–human CD45-APCCy7 conjugate (BD Biosciences), mouse anti–human CD73-PE (BD Biosciences), mouse anti–human CD90-PE (Chemicon–Merck Millipore), mouse anti–human CD133/1-Allophycocyanin (APC; Miltenyi Biotech), mouse anti–human CD163-PE (BD Biosciences), mouse anti–human CD56-PE (BD Biosciences), mouse anti–human CD3-PE (BD Biosciences), and mouse anti–human CD19 (Exbio Antibodies). Negative control samples were stained with the corresponding isotypes (mouse IgG1-PE, mouse IgG1-A PCCy7, and Alexa 488). All samples were analyzed on a flow cytometer (Epics XL; Beckman Coulter) with the use of System II software,

version 3.0 (Beckman Coulter). At least 1,000 cells in total were analyzed.

Xenotransplantation Assays with LGR5$^+$ Rhodamine$^+$ Cells

Animal care and use. All procedures involving animals in this study were approved by the Universidad de Valencia Institutional Review Board Ethics Committee (A1318591196411).

LGR5$^+$ cell labeling with the use of Molday ION Rhodamine. A non–transfection-based method, superparamagnetic iron oxide nanoparticle Molday ION Rhodamine B (SPIO) with fluorescent iron-oxide nanoparticles, was chosen to label endometrial cells for cell-tracking experiments in the in vivo model. Epithelial and stromal cells were plated in appropriate conditions with DMEM-F12 medium containing 10% FBS and 0.1% antibiotics and antimycotics (Gibco-Invitrogen) and incubated at 37°C and 5% CO_2. After cells adhered overnight, SPIO (CL-50Q02-6A-50 [2 mg Fe/mL]; Biopal) was added in different concentrations, 50 μg/mL for epithelial cells and 10 μg/mL for stromal cells, to the supplemented medium and samples were incubated for 22 hours. Neither stromal nor epithelial SPIO-labeled cells exhibited signs of cytotoxicity; stromal cell viability was ~91% and epithelial cell viability ~88% (data not presented). Rhodamine B fluorescence staining was analyzed with the use of a Cytomics FC500 cytometer (Beckman-Coulter) at 575 nm, determining that Rhodamine B labeling was 82%–93% in both stromal and epithelial cells.

Animal procedures. Female NOD-SCID mice (Nonobese diabetic/severe combined immunodeficient mice strain code 394, NOD CB17–Prkdc^{scid}/NCrCrl; Charles River Laboratories) were ovariectomized at 4–5 weeks to be used for xenotransplantation experiments (n = 6). The mice were treated with a cocktail of analgesic and antiinflammatory drugs and anesthetized with sevofluorane inhalation. Kidneys were externalized through a dorsal-horizontal incision to enable cell injection.

FACS-sorted LGR5$^+$ Rhodamine$^+$ single-cell suspensions (2,000–20,000 cells) were resuspended in 30 μL medium (DMEM-F12) and injected under the kidney capsule (n = 3) on the left side. The same number of LGR5$^-$ Rhodamine$^+$ cells were injected into the left kidney capsule of control mice (n = 3), this control was used to demonstrate the low reconstruction ability of LGR5$^-$ cells to give rise to endometrial-like tissue in vivo. Before the cell injection, both ovaries were removed to eliminate the influence of endogenous hormones. During transplantation, E_2 pellets (0.36 mg/60 days 17β-E_2, SE121; Innovative Research of America) were implanted in the neck, and after a 3-week period (only with E_2) P (provided by Dr. Carreras, Hospital 14, Barcelona) was administered subcutaneously every day for 2 weeks; after a second 3-week period (only with E_2) the mice were subjected to a second cycle of daily P injections for 2 more weeks. The hormonal treatment was administered to mimic human menstrual cycles in the injected mice. Throughout this experiment, xenotransplanted mice were maintained in a specific pathogen-free facility and fed ad libitum for 60 days after the initial cell injection. Subsequently, the mice were killed by inhalation of carbon dioxide (CO_2) and nephrectomized. Finally, the xenotransplanted kidneys were extracted, formalin fixed, and paraffin embedded.

Histological Analysis and Immunostaining

Detection of iron deposits. Paraffin sections from the injected kidneys were deparaffinized at 60°C and rehydrated through graded ethanol to distilled water. Accustain Iron Stain (procedure no. HT20; Sigma-Aldrich) was used to visualize the presence of iron deposits inside cells after treatment with Molday ION using Prussian Blue, according to the manufacturer's protocol. Mounted sections were visualized with a Nikon Eclipse 80i microscope with ×20, ×40, and ×63 objectives. The control samples used for iron deposits were the noninjected kidney as negative and the spleen as positive (because iron deposition usually occurs in the cells of the reticuloendothelial system).

Immunohistochemistry for endometrial SSC markers. Sections were deparaffinized and rehydrated through graded ethanol, rinsed in distilled water, and treated with antigen retrieval. Membrane permeabilization was performed for vimentin (Vm) staining. After blocking by means of PBS (5% BSA, 0.05% Tween-20), primary antibodies were added: mouse monoclonal anti–human CD9 (dilution 1:20, Abcam 49325) and mouse monoclonal anti–human Vm clone V9, (dilution 1:100, Dako M0725) for endometrial epithelial and stromal cells, respectively. A biotin-streptavidin kit was used for secondary antibody binding according to the manufacturer's instructions (LSAB method; Dakocytomation). Finally, detection was performed with the use of 3,3-diaminobenzidine incubation. Counterstained sections with hematoxylin were visualized with the use of a Nikon Eclipse 80i microscope with ×20, ×40, ×63, and ×100 objectives. The control samples used were the noninjected kidney as negative and the endometrium as positive.

Human Endometrial LGR5$^+$ Cell Transcriptome

RNA isolation and microarray hybridization. Total RNA was extracted from the isolated cell fractions by means of flow cytometry with the use of a Quick-RNA Microprep Kit (Zymo Research) according to the manufacturer's protocol. Quality of RNA was assessed with the use of RNA Pico Chips (Agilent Technologies). Each sample in this study consisted of a pool of four human endometrial biopsies. Four fractions each were selected from the stromal compartment (stromal LGR5$^+$ [n = 4] and stromal LGR5$^-$ [n = 4]) and three fractions each from the epithelial compartment (epithelial LGR5$^+$ [n = 3] and epithelial LGR5$^-$ [n = 3]); fractions were hybridized after fulfilling the required RNA quality standards.

Approximately 50 ng per sample was hybridized on the Human GE 4×44K v2 Microarray (Agilent Technologies), which targets 27,958 Entrez Gene RNAs, protocols were carried out according to the manufacturer's instructions. Hybridized microarrays were subsequently scanned with the use of a Power Scanner (Tecan).

Preprocessing, normalization, and differentially expressed genes in LGR5$^+$ cells. Gene expression array spot intensity measurements were performed with the use of the Genepix Pro 6.0 (Molecular Devices). Densitometry values were normalized to rule out possible sources of variation coming from nonbiologic sources by means of a quantile method and then further transformed to the logarithmic scale (log2).

Gene expression profiles were determined by comparing the experimental groups (LGR5$^+$ population) with the control group (LGR5$^-$ population) by means of nonparametric tests with the use of the Bioconductor package Rankprod (www.bioconductor.org) in R software (www.r-project.orf/). Up- and down-regulated genes in LGR5$^+$ cells were identified with the use of two criteria: an absolute fold change of ≥ 2.0, and a corresponding adjusted *P* value of $< .05$. To compare LGR5$^+$ cells in stromal and epithelial fractions, intersected genes were obtained with the use of the Venny tool (http://bioinfogp.cnb.csic.es/tools/venny/index.html).

Functional transcriptomic characterization of LGR5$^+$ cells. To understand the functional meaning of LGR5$^+$ cells' transcriptome, functional enrichment of differentially expressed genes in epithelial and stromal fractions were performed with the use of Clusterprofiler version 2.2.2 (22) from Bioconductor (release 3.1). Enriched terms for KEGG pathways (23) and Gene Ontology (www.geneontology.org/) were calculated by means of a gene set enrichment analysis (GSEA) ranking genes by fold-change values. We used the Benjamini-Hochberg conventional multiple-testing *P* value correction procedures (24) to derive adjusted *P* values.

Array validation. To verify the microarrays results, real-time polymerase chain reaction (PCR) was conducted with the use of three genes selected for validation: *IL1B* (interleukin-1β) and *CSF1R* (colony-stimulating factor 1 receptor), representing two up-regulated genes in the LGR5$^+$ population, and the down-regulated gene *RAMP1* (receptor activity–modifying protein 1). Designed primer pairs were: *IL1B*, forward TTACAGTGGCAATGAGGATG, reverse GTAGTGGTGGTCG GAGATTC; *RAMP*, forward CTAACTACGGTGCCCTCCT, reverse CTGTAGCTCCTGATGGTCCT; and *CSF1R*, forward GAGATGAGGCCTGTCTCCA, reverse ATGACCATTGGTCAA CAGCA. Real-time PCR was performed on the Roche Lightcycler 480 with the use of the Fast Start DNA Master Sybr-green I system (Roche) according to the manufacturer's protocol. The transcript levels were normalized to the *18S* gene for quantitative comparisons between different samples.

Comparative Analysis of LGR5$^+$ CD45$^+$ versus LGR5$^+$ CD45$^-$ Cells

Endometrial biopsies (n = 3) were sorted with the use of the BD FACS ARIA I instrument among three paired samples of LGR5$^+$ CD45$^+$ and LGR5$^+$ CD45$^-$ cells from each donor. Antibodies and protocols against LGR5 and CD45 and the staining procedure have been previously described (Novus and BD Biosciences). The secondary antibodies were Alexa647 and Alexa488, respectively. High-throughput RNA sequencing of the six samples was performed. Samples were processed on the Illumina platform RS-122-2301 with the use of Truseq Stranded Total RNA LT and the Ribo-Zero Gold Set A kit. A total of six paired-end (2 × 50) pairs of FASTQ files were obtained and analyzed. Basic quality controls were completed with FASTQC, FASTX-Toolkit, and PRINSEQ (25). Paired-end (forward-reverse) sample merging, as well as the remaining steps of the bioinformatics analysis, was performed with the software CLCBio Genomics Workbench version 8.0.2. Alignment and mapping were analyzed against the current human genome (*Homo sapiens* hg19 at both gene- and mRNA-level tracks, from Ensembl's Homo_sapiens.GRCh37.75.gtf.gz file). Counts were normalized by means of the standard RPKM method (26). Significance testing for differentially expressed genes was implemented with the use of Edge testing (27) (equivalent to F tests and *t* tests) within the same CLCBio software, with a significance criteria of alpha = .05, with adjustment for multiple testing with the false discovery rate method. Biologic significance analysis was performed by comparing gene set enrichment analysis against KEGG and GO (www.geneontology.org/) databases with the use of GAGE (28) and Pathview (29) Bioconductor packages.

RESULTS

Isolation and Immunophenotype Characterization of Human Endometrial LGR5$^+$ Cells

A total of 15 paired samples from the endometrial epithelial and stromal compartments was sorted for LGR5$^+$ cells (Fig. 1A). They represented an average 1.08 ± 0.73% of the cells in the epithelium, with 56.4% viability, and an average 0.82 ± 0.76% of the cells in the stromal compartment, with 60.2% viability.

The inmunophenotypic characterization of the isolated endometrial LGR5$^+$ revealed that they were negative for CD31 (mature endothelial cells), CD133 (endothelial progenitor cells), and CD34 (hematopoietic stem cells) in both endometrial cell fractions (Fig. 1B). Raw data of the percentages corresponding to cells stained for each marker are presented in Figure 1C. Surprisingly, we observed that 62.73% of epithelial LGR5$^+$ cells and 57.84% of stromal LGR5$^+$ cells were also CD45$^+$ (Fig. 1B and C). Whereas epithelial LGR5$^+$ cells showed low signal for CD73 and CD90 (<8%), stromal cells displayed a positive expression for these markers, ranging from 10% to 60% (Fig. 1B and C).

Owing to the unexpected abundance of CD45$^+$ marker in the LGR5$^+$ subpopulation, coexpression with other hematopoietic antigens was assessed. LGR5$^+$ CD45$^+$ cells (~48%) were positive for CD163 in epithelium; the same population represented >55% of cells in the stroma (Fig. 1B). LGR5$^+$ CD45$^+$ cells were negative for CD3, CD19, and CD56, revealing an unexpected association with macrophage origin but not with T lymphocytes, B lymphocytes, or natural killer uterine cells, respectively (Supplemental Fig. 1; Supplemental Figs. 1–5 are available online at www.fertstert.org).

Xenotransplantation Assays

To determine if the LGR5$^+$ Rhodamine$^+$ cell population was involved in the human endometrial-like tissue formation

FIGURE 1

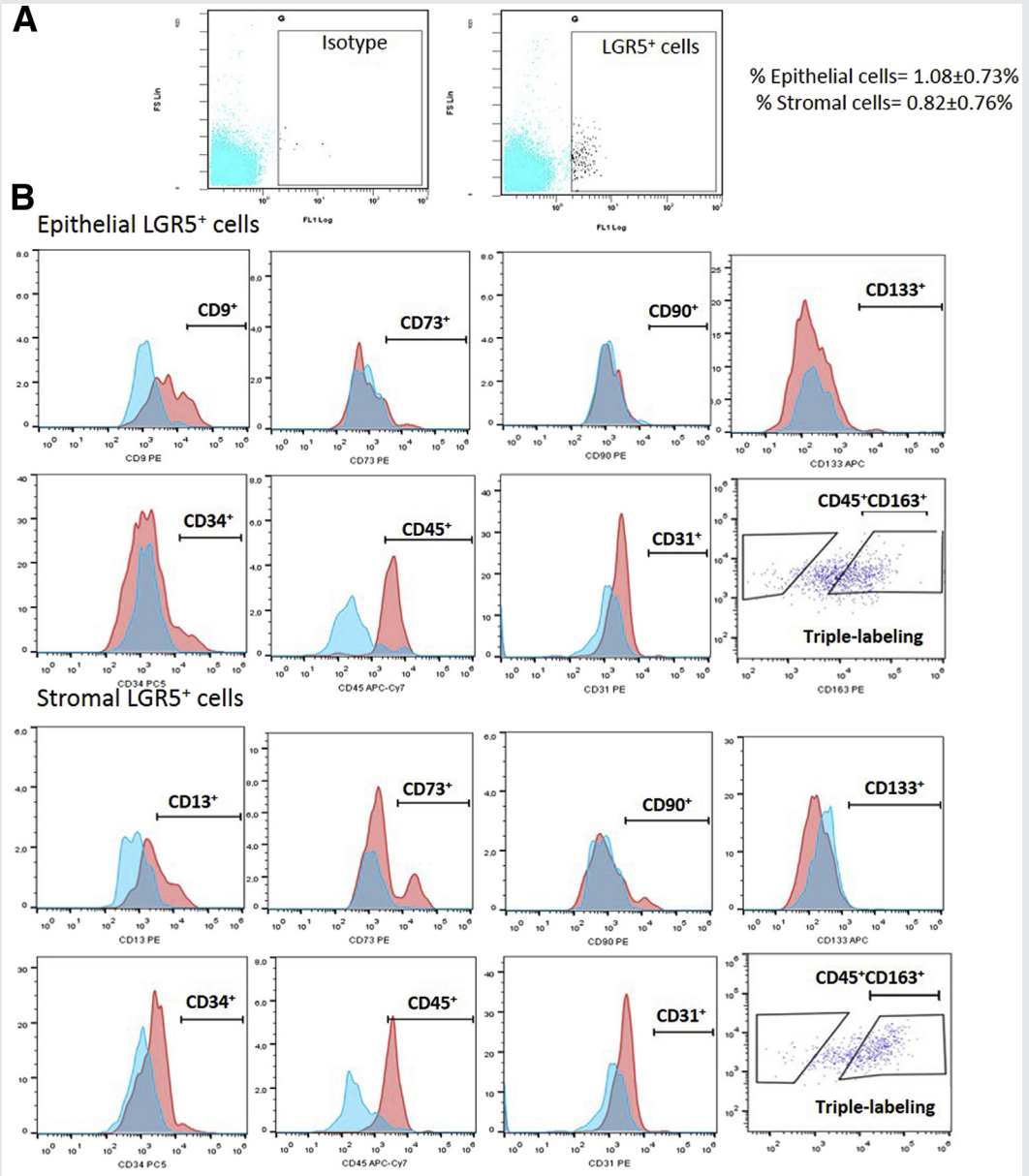

C

Markers	Epithelial Cells	Stromal Cells
LGR5⁺/CD9⁺	33.00 ± 12.39%	X
LGR5⁺/CD13⁺	X	30.05 ± 22.13%
LGR5⁺/CD31⁺	0%	0%
LGR5⁺/CD133⁺	0.19 ± 0.29%	0.54 ± 0.54%
LGR5⁺/CD34⁺	1.91 ± 1.3%	1.93 ± 1.3%
LGR5⁺/CD45⁺	62.73 ± 10.12%	57.84 ± 15.72%
LGR5⁺/CD73⁺	7.86 ± 7.28%	14.46 ± 15.43%
LGR5⁺/CD90⁺	5.68 ± 6.85%	17.19 ± 17.16%

Molecular phenotypic profile of the LGR5-expressing cells in human endometrium. (**A**) Representative fluorescence-activated cell sorter plot showing endometrial LGR5 staining. (**B**) Flow cytometric analysis of LGR5^{+} cells in the epithelial and stromal fractions of the human endometrium. Histograms showing specific coexpression of LGR5^{+} cells with several mesenchymal (CD90 and CD73), hematopoietic (CD34, CD45, and CD163), endothelial (CD31), and stem cell (CD133) markers. Bars indicate positive staining for each marker compared with isotype control samples. (**C**) Table summarizing the percentage of positive cells obtained by means of flow cytometry (n = 3–7 samples) for LGR5^{+} cells with different surface markers: CD9, CD13, CD31, CD133, CD34, CD45, CD73, and CD90.

Cervelló. LGR5⁺ cells in human endometrium. Fertil Steril 2016.

FIGURE 2

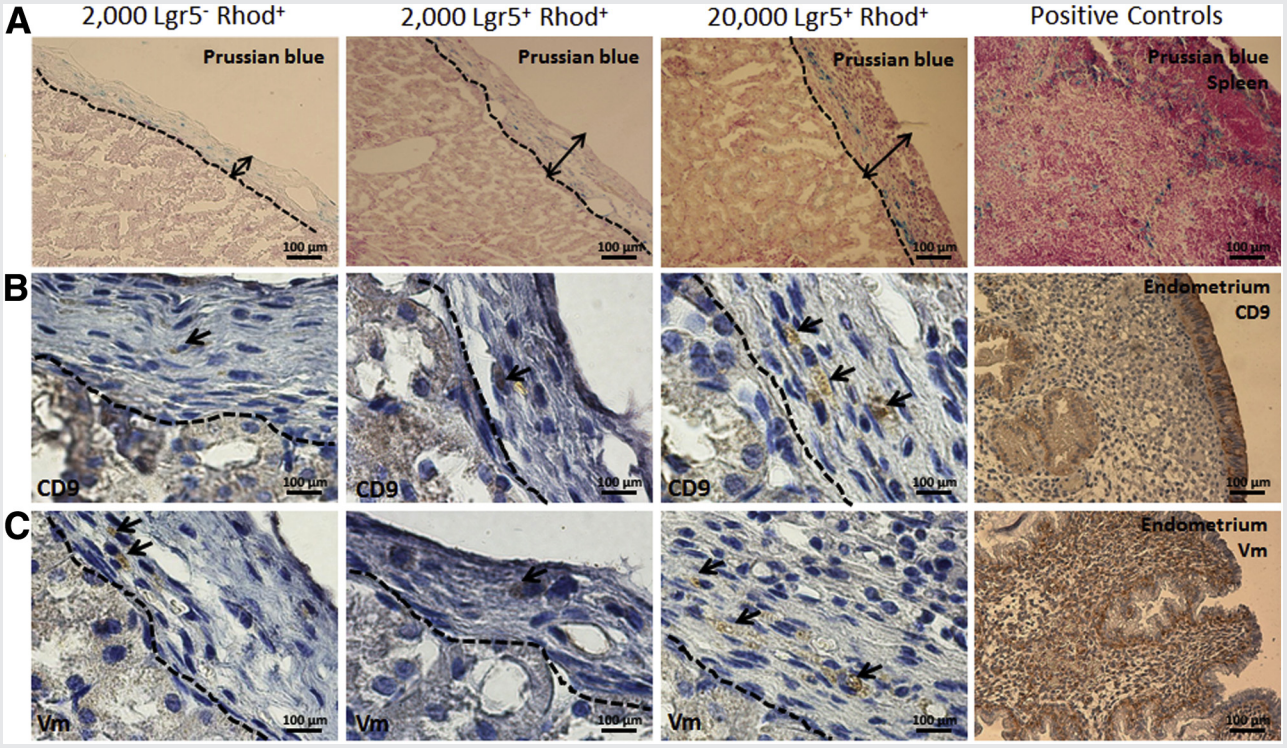

Representative sections from the left kidneys of three xenotransplanted mice are shown with (**A**) Prussian blue staining and (**B**) CD9 and (**C**) vimentin (Vm) immunohistochemistry. Control samples are shown in the last column: spleen for Prussian blue and endometrium for CD9 and Vm. Images were taken at ×40 and ×100 magnification. A *dashed line* delineates the kidney structure from the endometrial-like newly formed tissue. Positive staining for Prussian blue, shown by *blue spots*, suggests that newly formed endometrial tissue was developed from the human injected cells (*arrows*). Immunohistochemical analysis for human endometrial markers CD9 (epithelium) and Vm (stroma) was performed to test if the newly formed tissue had endometrial-like characteristics.

Cervelló. LGR5⁺ cells in human endometrium. Fertil Steril 2016.

in vivo, detection of iron deposits by means of Prussian blue staining and immunohistochemistry for endometrial SSC markers were performed. Furthermore, to characterize the new tissue present in the kidney capsule, immunohistochemistry for Vm and CD9 was performed.

After standardization of the protocol for staining with SPIOs in cultured endometrial cells (Supplemental Fig. 2), a total of 2,000, 4,000, and 20,000 each of LGR5$^+$ Rhodamine$^+$ (+/+) and LGR5$^-$ Rhodamine$^+$ (−/+) cells were injected under the kidney capsule of recipient mice (n = 6). Unfortunately, mice receiving 4,000 −/+, 20,000 −/+, and 20,000 +/+ cells died during the 3-month experimental period; only results obtained from the remaining animals (n = 3) are shown in Figure 2.

All three kidneys showed the presence of human cells within the kidney capsule. These results suggest that endometrial-like cells were regenerated from both LGR5$^+$ and LGR5$^-$ Rhodamine$^+$ endometrial fractions injected into the xenograft.

Transcriptomic Characterization

The transcriptomic signature of the LGR5$^+$ cell population of the human endometrium was generated with the use of epithelial (n = 3) and stromal (n = 4) LGR5$^+$ cells versus their corresponding LGR5$^-$ cells from both compartments. In total, 1,053 genes were differentially expressed in the epithelium and 679 in the stroma. Among these, 368 genes were common between both compartments, 681 were differentially expressed only in epithelium, and 307 only in stromal LGR5$^+$ cells. Moreover, the differential expression analysis, with the use as threshold of fold change ≥ 2.0 with $P<.05$, showed a total of 494 up- and 559 down-regulated genes in the LGR5$^+$ versus LGR5$^-$ epithelial cell fraction; and 619 up- and 60 down-regulated genes in the LGR5$^+$ versus LGR5$^-$ cells of the stromal fraction (Supplemental Fig. 3).

Functional analysis indicates that, independently from their stromal or epithelial origin, LGR5$^+$ cells share similar functional genomics and could therefore provide a global endometrial LGR5 cell signature. Using the enrichment score values from the gene set enrichment analysis, the main represented KEGG functions for both origins were organized based on the adjusted P value of $<.05$ (Fig. 3). Hematopoietic lineage (hsa04640) was in the top enrichment score for both compartments (epithelium, Fig. 3A; stroma, Fig. 3B). Interestingly, all the genes prevailing in this function were up-regulated and were represented in all the different subpathways

FIGURE 3

A GSEA LGR5⁺ Epithelial Cells

KEGG id	KEGG name	Gene Ratio	Background Ratio	Adjusted p-value	Enrichment score
hsa04612	Antigen processing and presentation	20/406	77/7011	0.0089	0.9117
hsa04640	Hematopoietic cell lineage	21/406	88/7011	0.0089	0.8873
hsa04514	Cell adhesion molecules (CAMs)	27/406	142/7011	0.0089	0.8530
hsa04010	MAPK signaling pathway	18/406	257/7011	0.0222	0.8525
hsa04620	Toll-like receptor signaling pathway	18/406	106/7011	0.0286	0.8415
hsa04380	Osteoclast differentiation	33/406	132/7011	0.0222	0.8104
hsa04060	Cytokine-cytokine receptor interaction	29/406	265/7011	0.0416	0.8000

B GSEA LGR5⁺ Stromal Cells

KEGG id	KEGG name	Gene Ratio	Background Ratio	Adjusted p-value	Enrichment score
hsa04640	Hematopoietic cell lineage	19/315	88/7011	0.0103	0.8842
hsa04010	MAPK signaling pathway	17/315	255/7011	0.0301	0.8523
hsa04612	Antigen processing and presentation	23/315	77/7011	0.0301	0.8498
hsa04620	Toll-like receptor signaling pathway	21/315	106/7011	0.0163	0.8442
hsa04514	Cell adhesion molecules (CAMs)	28/315	142/7011	0.0103	0.8306
hsa04060	Cytokine-cytokine receptor interaction	31/315	265/7011	0.0103	0.8084
hsa04145	Phagosome	41/315	88/7011	0.0103	0.8062

LGR5$^+$ cell gene set enrichment analysis (GSEA). Enriched KEGG functions in LGR5$^+$ cells isolated from (**A**) endometrial epithelial cells and (**B**) endometrial stromal cells. LGR5$^+$ cells were associated with hematopoietic cell lineage KEGG pathway (Supplemental Fig. 4; www.genome.jp/kegg-bin/show_pathway?hsa04640). The most enriched pathways (adjusted $P<.05$) and enrichment scores are presented. Enriched pathway in both epithelium and stroma is indicated by blue and yellow, respectively.

Cervelló. LGR5⁺ cells in human endometrium. Fertil Steril 2016.

(Supplemental Fig. 4), suggesting the implication of these LGR5$^+$ cells in the hematopoietic stem cell lineage.

The 24 differentially regulated genes are included in the hematopoietic pathway and are detailed in Supplemental Figure 5 as well as other genes related to interleukins, CD family, and major histocompatibility complex.

Profiles of LGR5$^+$ CD45$^+$ versus LGR5$^+$ CD45$^-$ Cells according to RNA Sequencing

Although differences between these two LGR5$^+$ subpopulations were found, no transcripts with false discovery rate <0.05 were observed (data not presented). We next selected top genes by means of unadjusted $P<.05$ and fold change >2.0. A total of 279 down-regulated transcripts were found, and the related pathways implicated were involved in chemokine signaling, cell cycle, endocytosis, apoptosis, Toll-like receptor signaling, and embryo development.

DISCUSSION

In previous work, we confirmed the existence of LGR5 expression in the human endometrium throughout the menstrual cycle, describing its localization in a restricted epithelial and stromal area located in the perivascular regions of the lower functionalis (19). In the present work, we isolated

FIGURE 4

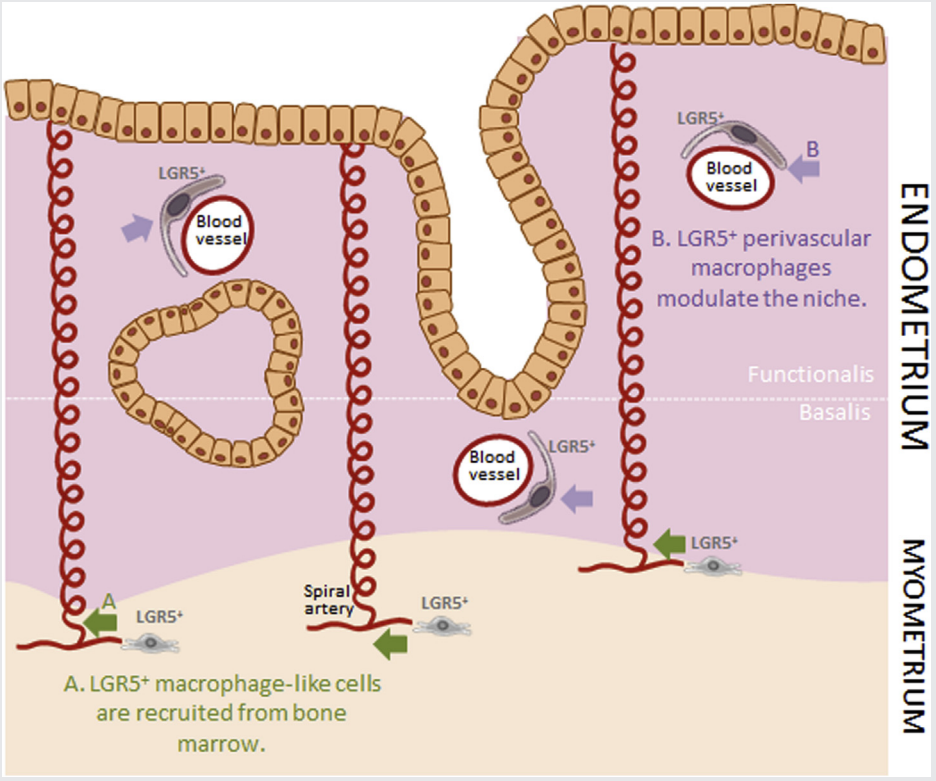

Schematic illustration of proposed hypotheses to describe the function of human endometrial LGR5$^+$ macrophage-like cells with hematopoietic origin. (**A**) LGR5$^+$ macrophage-like cells are recruited via bone marrow; and (**B**) LGR5$^+$ perivascular macrophages modulate the niche.

Cervelló. LGR5$^+$ cells in human endometrium. Fertil Steril 2016.

LGR5$^+$ cells from the human endometrium; the percentages of LGR5$^+$ cells isolated (0.8%–1%) are similar to the 0.6% LGR5$^+$ expressing cells isolated from the hair bulge (30). The existence of this rare subpopulation in the human endometrium was the first hint to consider LGR5$^+$ cells as a putative stem cell population (31).

The characterization of endometrial LGR5$^+$ cells reveals the absence of an endothelial, mesenchymal, or pure hematopoietic profile, but the presence of high CD45 expression. Clever's group also identified CD45$^+$ cells in an LGR5$^+$ hematopoietic stem cell fraction during mouse embryonic development and, consistently with our study, found that these cells reconstituted hematopoietic lineages in adult mice after transplantation although with very low efficiency (32). Moreover, the comparison of the gene expression profile of the positive and negative populations for CD45 (LGR5$^+$ CD45$^+$ versus LGR5$^+$ CD45$^-$) revealed no significant differences between the subpopulations despite the small number of samples assessed (n = 3).

Nevertheless, the coexpression of CD45 and CD163 in LGR5$^+$ cells indicates that this population is phenotypically similar to macrophages, which was unexpected. Macrophages have been implicated in processes such as tissue repair and remodeling (33). Most importantly, macrophages regulate adult stem cell niches such as the hematopoietic system (34), mammary gland (35), liver (36), and hair follicle (37), raising a new putative role for this subset of cells as niche gatekeepers (Fig. 4).

Macrophages have different roles according to their tissue microenvironment. In the hair follicle, macrophages display increased expression levels of Wnt ligands before the onset of the anagen phase, or growth phase, activating the epithelial stem cells in a Wnt-dependent manner to enter into anagen (37). Along this line, Wattananit et al. demonstrated that macrophage-like cells recruited from the blood are important in long-term spontaneous functional tissue recovery after ischemic brain injury (38).

To assess the potential of LGR5$^+$ cells for differentiation, xenotransplantation of cells was performed under the kidney capsule in immunocompromised mice. New putative endometrial-like tissue, which positively stained for Prussian blue as a reporter of human endometrial LGR5$^+$ cells, formed above the kidney capsule for both LGR5$^+$ and LGR5$^-$ cell fractions. The macroscopic appearance (morphology and thickening) of the reconstructed endometrial tissue was not like previous results in the in vivo nonhuman animal model (7–11), suggesting that we likely did not isolate a pure SSC population. Indeed, the reconstitution ability was very low, and a clear limitation is not only the low number of cells injected (2,000 and 20,000), but also the low efficiency of

LGR5$^+$ cells to reconstitute original cell lineages after transplantation (corroborated by Clever' s group in 2014 [32]).

The shared functions and the significant amount of shared genes (368) between LGR5$^+$ stromal and epithelial cells point to a substantial similarity and common cell fate between these two cell populations, postulating the similar origin for these endometrial LGR5$^+$ cells as a possible explanation. When we performed the functional analysis of the 368 common genes, the hematopoietic lineage showed a significant adjusted *P* value ($<.05$). The gene expression analysis further supports the presence of the CD45 marker in the LGR5$^+$ cells, suggesting an important role for LGR5-CD45 coexpression in the human endometrium.

The present data describe endometrial LGR5$^+$ cells as a rare population of cells with a low ability to form endometrial-like tissue and a phenotype closer to macrophages than to mesenchymal stem cells, thereby questioning the utility of LGR5 as a specific marker for endometrial stem cells. These data suggest that endometrial LGR5$^+$ cells may instead be a resident component displaying macrophage features within the niche located in the perivascular microenvironment (39). It is well known that macrophages interact with stem cells within their specific niche to modulate self-renewal and tissue remodeling (40).

The principal limitations of this study are the relatively small sample size of xenograft assays owing to the difficulties raised by the experimental animal model; nevertheless, we were able to corroborate our hypothesis and results through several complementary assays.

In conclusion, we propose two hypotheses to explain the potential role of LGR5$^+$ cells in the human endometrial stem cell niche: 1) After tissue damage during menstruation, the perivascular macrophages mobilize surrounding stem cells to respond to the injury for repair and remodeling of a new endometrial layer; tissue-resident macrophages described here could be part of the different components of the endometrial stem cell niche; or 2) in the endometrium these macrophage-like cells are naturally recruited from an exogenous source, such as bone marrow, to activate the endogenous niche, thereby contributing to long-term functional recovery (41).

Acknowledgments: The authors thank Dr. Juan Manuel Moreno and Dra. Aymara Mas from Fundación IVI for the scientific support; and Sebastian Martínez for his technical support. High-throughput RNA sequencing statistical analysis was carried out in the Statistics and Bioinformatics Unit of the Vall Hebron Institute of Research.

REFERENCES

1. Prianishnikov VA. On the concept of stem cell and a model of functional-morphological structure of the endometrium. Contraception 1978;18:213–23.
2. Padykula HA. Regeneration in the primate uterus: the role of stem cells. Ann N Y Acad Sci 1991;622:47–56.
3. Chan RW, Schwab KE, Gargett CE. Clonogenicity of human endometrial epithelial and stromal cells. Biol Reprod 2004;70:1738–50.
4. Cervelló I, Simón C. Somatic stem cells in the endometrium. Reprod Sci 2009;16:200–5.
5. Kato K, Yoshimoto M, Kato K, Adachi S, Yamayoshi A, Arima T, et al. Characterization of side-population cells in human normal endometrium. Hum Reprod 2007;22:1214–23.
6. Tsuji S, Yoshimoto M, Takahashi K, Noda Y, Nakahata T, Heike T. Side population cells contribute to the genesis of human endometrium. Fertil Steril 2008;90:1528–37.
7. Cervelló I, Gil-Sanchis C, Mas A, Delgado-Rosas F, Martínez-Conejero JA, Galán A, et al. Human endometrial side population cells exhibit genotypic, phenotypic and functional features of somatic stem cells. PLoS One 2010;5:e10964.
8. Masuda H, Matsuzaki Y, Hiratsu E, Ono M, Nagashima T, Kajitani T, et al. Stem cell-like properties of the endometrial side population: implication in endometrial regeneration. PLoS One 2010;5:e10387.
9. Cervelló I, Mas A, Gil-Sanchis C, Peris L, Faus A, Saunders PT, et al. Reconstruction of endometrium from human endometrial side population cell lines. PLoS One 2011;6:e21221.
10. Schwab KE, Gargett CE. Co-expression of two perivascular cell markers isolates mesenchymal stem-like cells from human endometrium. Hum Reprod 2007;22:2903–11.
11. Götte M, Wolf M, Staebler A, Buchweitz O, Kelsch R, Schring AN, et al. Increased expression of the adult stem cell marker Musashi-1 in endometriosis and endometrial carcinoma. J Pathol 2008;215:317–29.
12. Masuda H, Anwar SS, Bühring HJ, Rao JR, Gargett CE. A novel marker of human endometrial mesenchymal stem-like cells. Cell Transplant 2012;21:2201–14.
13. van der Flier LG, Sabates-Bellver J, Oving I, Haegebarth A, de Palo M, Anti M, et al. The intestinal Wnt/TCF signature. Gastroenterology 2007;132:628–32.
14. Barker N, van Es JH, Kuipers J, Kujala P, van den Born M, Cozijnsen M, et al. Identification of stem cells in small intestine and colon by marker gene LGR5. Nature 2007;449:1003–7.
15. Barker N, van Es JH, Jaks V, Kasper M, Snippert H, Toftgård R, et al. Very long-term self-renewal of small intestine, colon, and hair follicles from cycling Lgr5+ve stem cells. Cold Spring Harb Symp Quant Biol 2008;73:351–6.
16. Morris RJ, Liu Y, Marles L, Yang Z, Trempus C, Li S, et al. Capturing and profiling adult hair follicle stem cells. Nat Biotechnol 2004;22:411–7.
17. Barker N, Rookmaaker MB, Kujala P, Ng A, Leushacke M, Snippert H, et al. Lgr5(+ve) stem/progenitor cells contribute to nephron formation during kidney development. Cell Rep 2012;2:540–52.
18. Krusche CA, Kroll T, Beier HM, Classen-Linke I. Expression of leucine-rich repeat–containing G-protein–coupled receptors in the human cyclic endometrium. Fertil Steril 2007;87:1428–37.
19. Gil-Sanchis C, Cervelló I, Mas A, Faus A, Pellicer A, Simón C. Leucine-rich repeat–containing G-protein–coupled receptor 5 (Lgr5) as a putative human endometrial stem cell marker. Mol Hum Reprod 2013;19:407–14.
20. Gargett CE, Schwab KE, Deane JA. Endometrial stem/progenitor cells: the first 10 years. Hum Reprod Update 2016;22:137–63.
21. Simón C, Piquette GN, Frances A, Polan ML. Localization of interleukin-1 type I receptor and interleukin-1 beta in human endometrium throughout the menstrual cycle. J Clin Endocrinol Metab 1993;77:549–55.
22. Yu G, Wang L, Han Y, He Q. ClusterProfiler: an R package for comparing biological themes among gene clusters. OMICS 2012;16:284–7.
23. Kanehisa M, Goto S, Sato Y, Furumichi M, Tanabe M. KEGG for integration and interpretation of large-scale molecular data sets. Nucleic Acids Res 2012;40:D109–14.
24. Benjamini Y, Hochberg Y. Controlling the false discovery rate: a practical and powerful approach to multiple testing. J R Stat Soc B 1995;57:289–300.
25. Schmieder R, Edwards R. Quality control and preprocessing of metagenomic datasets. Bioinformatics 2011;27:863–4.
26. Aanes H, Winata C, Moen LF, Ostrup O, Mathavan S, Collas P, et al. Normalization of RNA-sequencing data from samples with varying mRNA levels. PLoS One 2014;9:e89158.
27. Carpendale S, Chen M, Evanko D, Gehlenborg N, Gorg C, Hunter L, et al. Ontologies in biological data visualization. IEEE Comput Graph Appl 2014;34:8–15.

28. Luo W, Friedman MS, Shedden K, Hankenson KD, Woolf PJ. GAGE: generally applicable gene set enrichment for pathway analysis. BMC Bioinformatics 2009;10:161.
29. Luo W, Brouwer C. Pathview: an R/Bioconductor package for pathway-based data integration and visualization. Bioinformatics 2013;29:1830–1.
30. Jaks V, Barker N, Kasper M, van Es JH, Snippert HJ, Clevers H, et al. Lgr5 marks cycling, yet long-lived, hair follicle stem cells. Nat Genet 2008;40:1291–9.
31. Li L, Clevers H. Coexistence of quiescent and active adult stem cells in mammals. Science 2010;327:542–5.
32. Liu D, He XC, Qian P, Barker N, Trainor PA, Clevers H, et al. Leucine-rich repeat–containing G-protein–coupled receptor 5 marks short-term hematopoietic stem and progenitor cells during mouse embryonic development. J Biol Chem 2014;289:23809–16.
33. Mantovani A, Biswas SK, Galdiero MR, Sica A, Locati M. Macrophage plasticity and polarization in tissue repair and remodelling. J Pathol 2013;229:176–85.
34. Chow A, Lucas D, Hidalgo A, Mendez-Ferrer S, Hashimoto D, Scheiermann C, et al. Bone marrow CD169+ macrophages promote the retention of hematopoietic stem and progenitor cells in the mesenchymal stem cell niche. J Exp Med 2011;208:261–71.
35. Gyorki DE, Asselin-Labat ML, van Rooijen N, Lindeman GJ, Visvader JE. Resident macrophages influence stem cell activity in the mammary gland. Breast Cancer Res 2009;11:R62.
36. Boulter L, Govaere O, Bird TG, Radulescu S, Ramachandran P, Pellicoro A, et al. Macrophage-derived Wnt opposes Notch signaling to specify hepatic progenitor cell fate in chronic liver disease. Nat Med 2012;18:572–9.
37. Castellana D, Paus R, Perez-Moreno M. Macrophages contribute to the cyclic activation of adult hair follicle stem cells. PLoS Biol 2014;12:e1002002.
38. Wattananit S, Tornero D, Graubardt N, Memanishvili T, Monni E, Tatarishvili J, et al. Monocyte-derived macrophages contribute to spontaneous long-term functional recovery after stroke in mice. J Neurosci 2016;36:4182–95.
39. Lane SW, Williams DA, Watt FM. Modulating the stem cell niche for tissue regeneration. Nat Biotechnol 2014;32:795–803.
40. Sainz B, Carron E, Vallespinós M, Machado HL. Cancer stem cells and macrophages: implications in tumor biology and therapeutic strategies. Mediators Inflamm 2016;2016:9012369.
41. Santamaria X, Cabanillas S, Cervelló I, Arbona C, Raga F, Ferro J, et al. Autologous cell therapy with CD133+ bone marrow–derived stem cells for refractory Asherman's syndrome and endometrial atrophy: a pilot cohort study. Hum Reprod 2016;31:1087–96.

SUPPLEMENTAL FIGURE 1

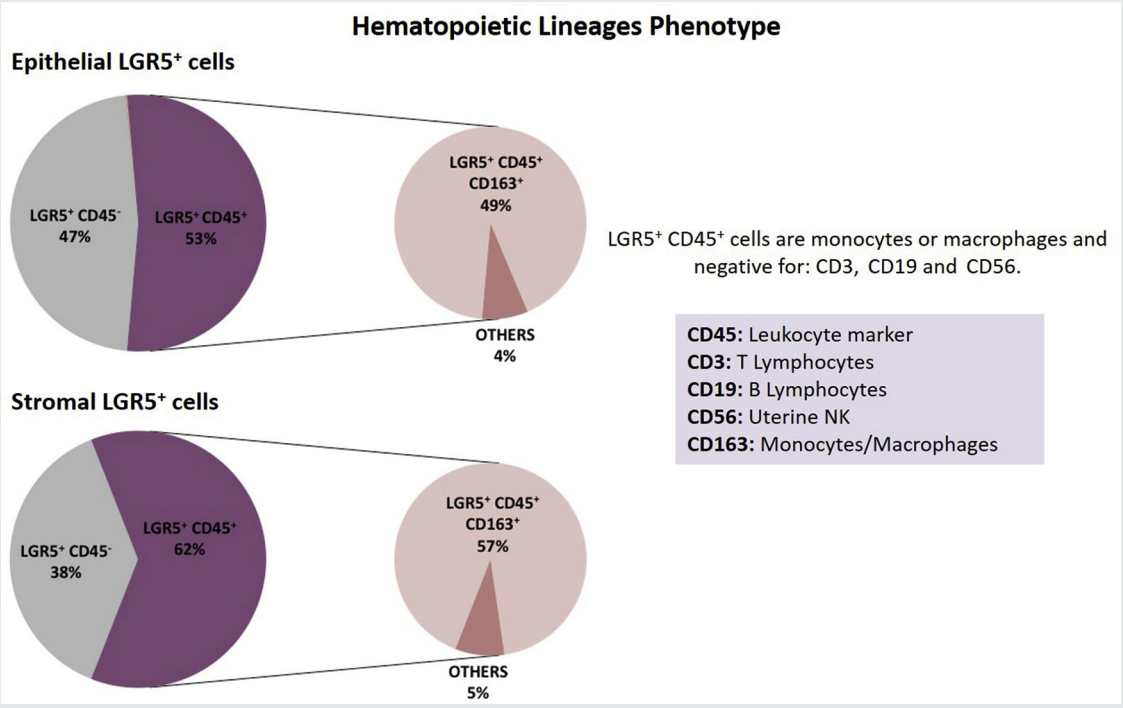

Diagram showing the specific phenotypes of LGR5^{+} cells related to hematopoietic lineage markers.

Cervelló. LGR5^{+} cells in human endometrium. Fertil Steril 2016.

SUPPLEMENTAL FIGURE 2

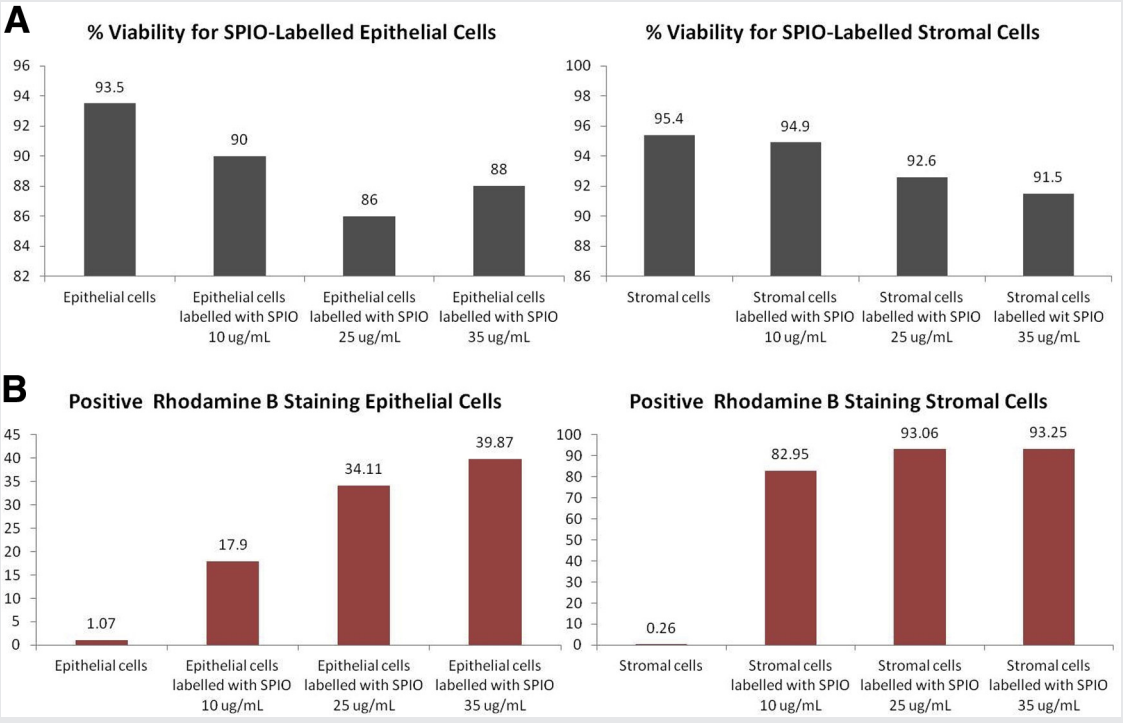

Results from the in vitro assays, showing the standardization of the superparamagnetic iron oxide nanoparticle (SPIO) protocol.

Cervelló. LGR5^{+} cells in human endometrium. Fertil Steril 2016.

SUPPLEMENTAL FIGURE 3

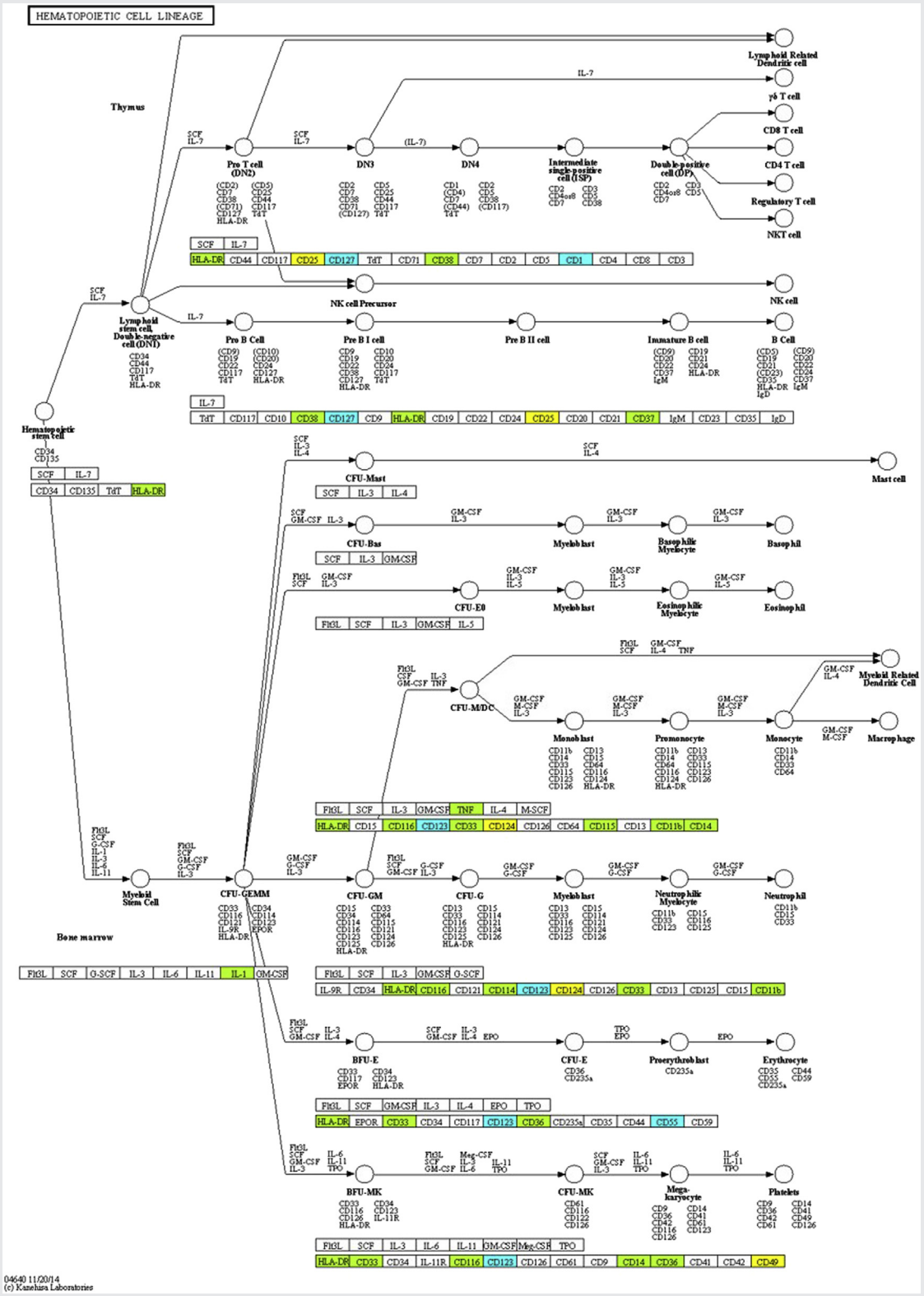

List of genes up- and down-regulated in the epithelial and stromal fractions of the LGR5^{+} cell populations of the human endometrium versus their whole epithelial and stromal counterparts (LGR5^{-}).

Cervelló. LGR5^{+} cells in human endometrium. Fertil Steril 2016.